

T. LEE<sup>1,✉</sup>  
W.G. BESSLER<sup>2</sup>  
C. SCHULZ<sup>3</sup>  
M. PATEL<sup>1</sup>  
J.B. JEFFRIES<sup>1</sup>  
R.K. HANSON<sup>1</sup>

## UV planar laser induced fluorescence imaging of hot carbon dioxide in a high-pressure flame

<sup>1</sup> High Temperature Gasdynamics Laboratory, Department of Mechanical Engineering, Stanford University, Stanford, CA 94305, USA

<sup>2</sup> Interdisciplinary Center for Scientific Computing (IWR), Universität Heidelberg, Im Neuenheimer Feld 368, 69120 Heidelberg, Germany

<sup>3</sup> Physikalisch-Chemisches Institut (PCI), Universität Heidelberg, Im Neuenheimer Feld 253, 69120 Heidelberg, Germany

Received: 19 May 2004

Published online: 29 July 2004 • © Springer-Verlag 2004

**ABSTRACT** UV planar laser-induced fluorescence (PLIF) images of hot carbon dioxide (CO<sub>2</sub>) are obtained in a laminar flame (CH<sub>4</sub>/air) at high pressure (20 bar) with excitation wavelengths at 239.34 nm and 242.14 nm. Excitation wavelengths are chosen to minimize the contribution of nitric oxide and molecular oxygen LIF signals. Spectrally resolved single point measurements are used for correction of the remaining oxygen LIF interference. The continuum LIF signal from electronically excited CO<sub>2</sub> is detected in a broad (280–400 nm) emission region. The UV PLIF of hot CO<sub>2</sub> has the potential for application to a wide variety of diagnostic needs in high-pressure flames, combustors, and engines.

PACS 42.62.Fi; 42.30.Va; 07.25+k; 39.30+w

### 1 Introduction

Laser-based detection of combustion species has proven to be an effective tool for combustion research [1–3]. These non-intrusive diagnostic techniques have proven quite useful for the optimization of practical combustion systems to minimize emissions and/or maximize combustion efficiency. Imaging measurements providing two-dimensional visualization of reactive species such as OH and CH or pollutant products such as NO have been especially useful in the development of modern high-pressure combustors such as those used in gas turbines [4] or internal combustion engines [5–7]. Although laser-induced fluorescence (LIF) imaging strategies exist for several important chemical intermediates, published strategies for planar laser-induced fluorescence (PLIF) of CO<sub>2</sub> are limited to infrared excitation and detection using vibrational transitions [8, 9]. Unfortunately, vibrational transitions have a complex energy transfer, ther-

mal emission is strong in the infrared, and modern high speed infrared camera technology is only emerging; thus, an ultraviolet (UV) method to visualize CO<sub>2</sub> is desirable.

At room temperature CO<sub>2</sub> is transparent for wavelengths above 200 nm, but at flame temperatures the absorption of hot, vibrationally excited CO<sub>2</sub> extends beyond 300 nm [10]. The importance of UV absorption by hot CO<sub>2</sub> for quantitative UV laser diagnostics in combustion systems was only recently recognized [11]. Subsequently, it was discovered that some of the CO<sub>2</sub> molecules excited by this absorption emit a broadband LIF with a faint, superimposed structure between 200 and 400 nm [12]. This broadband LIF emission was found to be present in spectrally-resolved measurements in CH<sub>4</sub>/air and CH<sub>4</sub>/Ar/O<sub>2</sub> flames at elevated pressures, where the intensity of the LIF signal varied with CO<sub>2</sub> absorbance and the lack of signal in a 20 bar H<sub>2</sub>/O<sub>2</sub>/Ar flame eliminated the possibility of LIF from H<sub>2</sub>O. That work

showed that the CO<sub>2</sub> signal was linear with number density and laser fluence within investigated ranges [12].

In this paper we report on the first UV LIF images of CO<sub>2</sub> in a laminar steady high-pressure flame (20 bar). Although these first images are not quantitative concentration maps of CO<sub>2</sub>, they illustrate the potential to image the distribution of hot exhaust gases in practical high-pressure combustors. Excitation wavelengths in this spectral region overlap with other species, notably A<sup>2</sup>Σ<sup>-</sup>-X<sup>2</sup>Π γ bands of NO and B<sup>3</sup>Σ<sup>-</sup>-X<sup>3</sup>Σ<sup>+</sup> Schumann-Runge bands of O<sub>2</sub> [13]. Contributions from NO can be avoided by selecting an excitation wavelength that does not overlap with any nearby NO transitions. However, due to the pervasive nature of multiple vibrational bands of O<sub>2</sub> in this region, it is impossible to avoid O<sub>2</sub>-LIF interference completely. Therefore, an O<sub>2</sub> signal subtraction scheme was implemented to ensure the purity of the CO<sub>2</sub>-LIF signal.

### 2 CO<sub>2</sub> UV planar laser induced imaging

#### 2.1 Experimental setup

To image CO<sub>2</sub> in high-pressure flames, a laminar, premixed methane/air flame was stabilized on a porous sintered stainless steel matrix of 8 mm in diameter. This facility has been previously used for measurements of NO-LIF at high-pressure [16]. The burner is mounted in a stainless steel housing with an inner diameter of 60 mm with pressure stabilization of ±0.1 bar. The flame is stabilized and the pressure is regulated primarily by a jet of secondary air around the cir-

✉ Fax: +1-650/723-1748, E-mail: Tonghun@Stanford.edu

cumference of the burner matrix. Investigations were conducted for  $\varphi = 1.1$  fuel/air equivalence ratio, where the uniform  $\text{CO}_2$  core region extends 5 mm vertically above the flame. Optical access to the flame was possible via quartz windows on all four sides of the burner housing. Laser light (2 mJ at 235–243 nm,  $0.25 \text{ cm}^{-1}$  FWHM) from a Nd:YAG-pumped (Quanta Ray GCR 250) frequency-doubled (BBO) dye laser (LAS, LDL205) was formed into a vertical light sheet ( $10 \times 0.5 \text{ mm}^2$ ) crossing the flame horizontally, where it illuminated a cross section through the center of the flame 1–10 mm above the burner matrix. The pulse energy was measured with a photodiode (LaVision). Fluorescence signals were collected at right angles to the laser beam and focused with a  $f = 105 \text{ mm}$ ,  $f/4.5$  achromatic UV-lens (Nikon) onto the chip of an intensified CCD camera (LaVision Dynamight). The signal light was discriminated against elastically scattered light with a 280 nm long-pass dielectric filter (Optosigma), and through an internal transmittance UV-transmitting bandpass filter (120 nm bandpass, center @340 nm, Optosigma). To quantify the  $\text{O}_2$ -LIF contribution in our images, a spectrometer (Chromex 250IS) was used with the camera for spectrally resolved detection of line images of  $\text{CO}_2$  and  $\text{O}_2$  LIF.

## 2.2 $\text{CO}_2$ UV-LIF image extraction

Detection of  $\text{CO}_2$  in high-pressure flames is complicated by the following issues. Excitation of  $\text{CO}_2$  in the 200–300 nm spectral region directly overlaps with excitation of the  $A^2\Sigma^- - X^2\Pi \gamma$  bands of NO and the  $B^3\Sigma^- - X^3\Sigma^+$  Schumann-Runge bands of  $\text{O}_2$ . Pressure broadening increases this overlap. Finding an excitation wavelength where both species are minimized is difficult due to the widely pervasive nature of  $\text{O}_2$  bands in this region [14]. We have chosen a strategy to use excitation wavelengths which avoid overlap with NO transitions in the region, while at the same time, minimizing the overlap with the multiple vibrational bands of  $\text{O}_2$ . Two candidate excitation wavelengths were selected, 239.34 nm and 242.14 nm, both of which are located between the  $A-X(0,1)$  and  $A-$

$X(0,2)$  bands of NO as shown in Fig. 1 (lower plot). These choices minimize contributions of  $\text{O}_2$  (Fig. 1, upper plot), as predicted by numerical simulations (LIFSim [15]), and also as confirmed through experimental excitation scans with wavelength-resolved detection in a lean high-pressure flame ( $\varphi = 0.8$ ,  $p = 10 \text{ bar}$ ), where excess  $\text{O}_2$  yields an identifiable LIF signal in the burnt gas. In comparison, excitation at 242.14 nm was found to provide the least interference from  $\text{O}_2$  with sufficient NO minimization, while 239.34 nm excitation is more selective in completely avoiding any NO transition.

The detection window of the  $\text{CO}_2$ -LIF signal extends from 280 to 400 nm.

This ensures suppression of Rayleigh scattering as well as Raman scattering from other combustion products. The 400 nm blue limit also suppresses background from flame emission, scattered pump-laser, and/or room light. Figure 2 shows a spectrally-resolved  $\text{CO}_2$  UV-LIF emission spectrum in the center region and outer edge of the flame. The spectral detection window is shown as a box in Fig. 2. The  $\text{CO}_2$ -LIF signal corresponds to the broadband signal evident throughout the entire detection region, although additional emission from  $\text{O}_2$  LIF appears as we move towards the outer rim of the flame where additional air is entrained and  $\text{O}_2$  levels are increased.

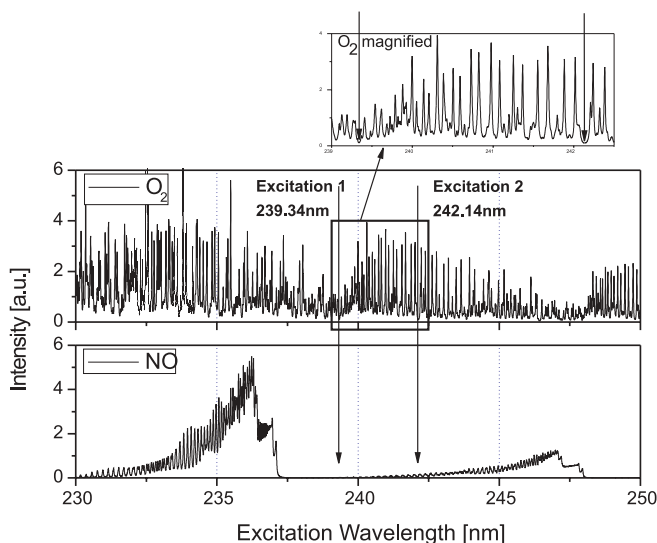


**FIGURE 1** Simulated LIF excitation spectra of  $\text{O}_2$  (upper frame) and NO (lower frame) at 20 bar and 2000 K (LIFSim [15]). A magnified  $\text{O}_2$  spectrum near the excitation wavelengths is also shown. 239.34 nm and 242.14 nm excitation lines are shown with arrows

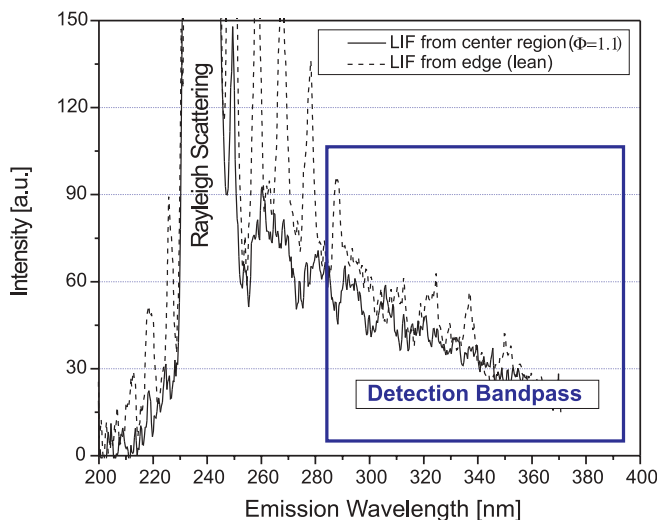


**FIGURE 2** Spectral detection bandpass (280–400 nm) shown on spectrally-resolved  $\text{CO}_2$  UV-LIF spectra with 242.14 nm excitation in the center and outer edge region of the flame

The resulting images are corrected for laser sheet inhomogeneities and the signal attenuation along the path of the laser beam caused by hot  $\text{CO}_2$  and  $\text{H}_2\text{O}$  absorption. Correction of attenuation utilizes recently quantified absorption cross-section data [11] of hot  $\text{CO}_2$  as well as flame temperatures obtained from multi-line fitting of NO-LIF excitation scans [16, 17] using LIFSim [15]. Additional correction for  $\text{O}_2$ -LIF contribution was carried out by taking spectrally resolved images and extracting the spatial distribution of  $\text{O}_2$  across the flame and subtracting it from the  $\text{CO}_2$ -LIF image. For this, spectrometer measurements were taken at a location 3 mm above the burner matrix using a beam instead of an expanded laser sheet. The slit of the spectrometer provides the spatial resolution across the horizontal span of the flame. The spatial distribution of  $\text{CO}_2$  across the flame can be extracted from the spectrally resolved images by assuming that the signal from the center region of the flame (Fig. 2, solid line) is mainly  $\text{CO}_2$ . As we move towards the edge of the flame, an additional  $\text{O}_2$ -LIF signal (dotted line) is observed and can be isolated to yield the amount of  $\text{O}_2$ -LIF interference. The  $\text{O}_2$ -LIF field was extrapolated to the remainder of the flame using geometrical arguments and assuming uniform composition of the burnt gas.

### 3 Results

$\text{CO}_2$  visualization using UV-LIF in a 20 bar flame along with signal attenuation along the path of the laser and  $\text{O}_2$  contribution information are presented in Fig. 3.

Signal attenuation across the centerline can amount to over 10% at 20 bar across a flame with an exit diameter of 8 mm [16]. As pressure increases, absorption cross-section data and experimental observations confirm that  $\text{CO}_2$  and  $\text{H}_2\text{O}$  absorption dominate and require significant correction for UV diagnostics below 250 nm [10, 16]. Other absorption mechanisms are not relevant in the flame under study (e.g. scattering loss from soot (in case of sooting flames,  $\varphi > 1.5$ ), absorption by PAH or by other molecules such as NO or  $\text{O}_2$ ). Although not required for our small flame, absorption of fluorescence signal radiating from the laser plane to the collecting

lens may also need to be considered. For the work reported here, attenuation corrections are made for the excitation laser beam using Beer-Lambert's law with absorption cross-section data. A pixel by pixel attenuation correction across the centerline of the flame is made and image b of Fig. 3 shows the magnitude of attenuation calculations.

The attenuation correction requires knowledge of the temperature field, which was determined for this flame using a multi-line NO-LIF temperature imaging technique [16], and is shown in image a of Fig. 3. UV LIF of  $\text{CO}_2$  proposed in this report only pertains to hot  $\text{CO}_2$  whose absorption cross-sections are sufficient for subsequent release of fluorescence photons. While this limits the detection of low temperature  $\text{CO}_2$ , it may provide an opportunity to directly infer temperature in combustion exhaust where uniform  $\text{CO}_2$  concentration assumptions can be made.

Images c and d show visualizations of the combined  $\text{CO}_2$  and  $\text{O}_2$ -LIF for

excitation at 239.34 nm and 242.14 nm, respectively. In addition, images e and f show the distribution of the  $\text{O}_2$ -LIF contribution for the respective excitation wavelength. The observed  $\text{O}_2$ -LIF contribution in the stable center region of the flame is around 1% of the entire LIF signal for our flame conditions (equivalence ratio of  $\varphi = 1.1$ ), which we attribute to noise in the extraction process. It can also be seen that the  $\text{O}_2$  concentration increases around the edges of the flame where air from the secondary flow is entrained into the system.

Images g and h of Fig. 3 shows the final  $\text{CO}_2$ -LIF distribution images using UV LIF with excitation at 239.34 nm and 242.14 nm respectively. It can be observed that  $\text{CO}_2$ -LIF intensities remain fairly constant to a first-order estimate throughout the hot burnt gas region. Previous studies with spectrally-resolved point measurements show that the relative contribution of  $\text{CO}_2$ -LIF signals increase with pressure and can become a significant interference source in

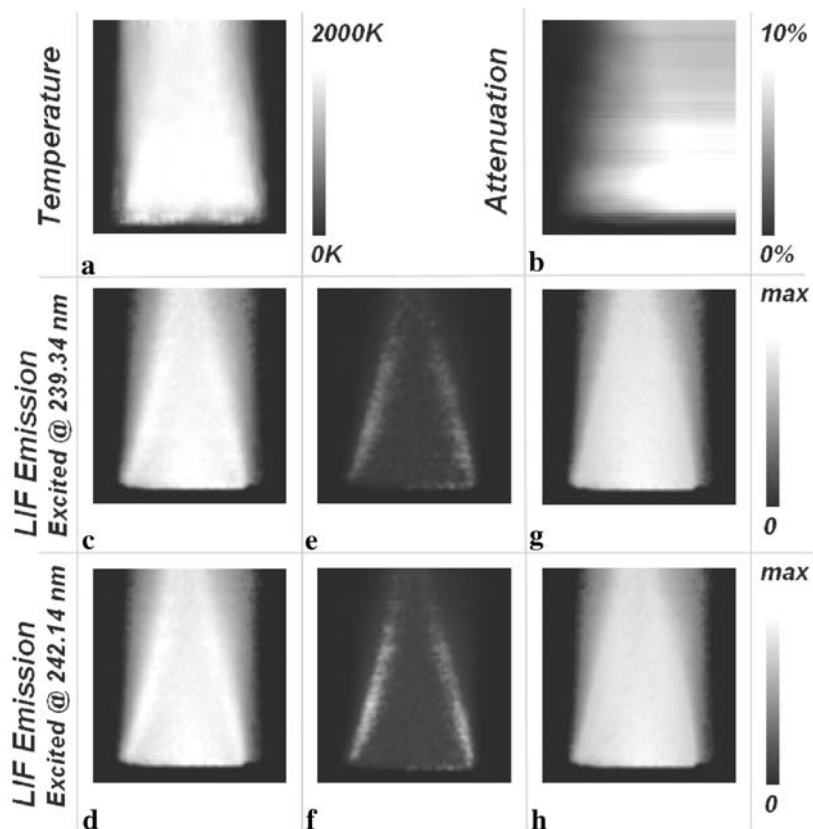


**FIGURE 3** Results of imaging analysis of  $\text{CO}_2$  UV-PLIF. **a** temperature field obtained from NO-LIF thermometry [15–17]. **b** total attenuation due to hot  $\text{CO}_2$  and  $\text{H}_2\text{O}$  (239.34 nm excitation); **c** and **d**  $\text{CO}_2$ -LIF and  $\text{O}_2$ -LIF combined image for 239.34 nm and 242.14 nm excitation, respectively; **e** and **f**  $\text{O}_2$ -LIF contribution for 239.34 nm and 242.14 nm excitation, respectively; **g** and **h** final  $\text{CO}_2$ -LIF image with  $\text{O}_2$ -LIF correction for 239.34 nm and 242.14 nm excitation, respectively. Images **c–h** share the same scale

detection of other minor species in post combustion gases [12].

The visualization of CO<sub>2</sub> is more accurate near the center of the burnt gas cone and becomes less reliable around the edges, because the laser sheet measurements access the burnt gas region above the flat flame, where only the central cone of the hot exhaust gas is stable; the outer part of the flame is increasingly unstable as density stratification occurs in the hot gas and Rayleigh instability forces an oscillation. Significant systematic errors affect signal interpretation in this fluctuating region. In addition, the temperature of the gas, which is quite uniformly hot in the center region, cools significantly around the edges due to the entraining effect of the co-flow air. The detection efficiency is less in this region as the UV absorption by CO<sub>2</sub> is quite temperature dependent.

In the earlier observation of CO<sub>2</sub> LIF [12], the variation of the CO<sub>2</sub> fluorescence signal was shown to vary linearly with pressure and laser fluence. This suggests that the excited state lifetime is limited by non-radiative, unimolecular loss processes, which may mitigate collisional quenching effects on the UV CO<sub>2</sub> PLIF.

#### 4 Conclusion

We present 2D-LIF images of hot CO<sub>2</sub> using UV excitation in the burnt gases of a premixed, high-pressure laminar flame. To our knowledge, these are the first CO<sub>2</sub> images published using UV excitation and detection. Excitation at 239.34 nm and 242.14 nm can effectively avoid overlap with NO transitions

in the region, while at the same time, minimize overlap with the multiple vibrational bands of O<sub>2</sub>. A first-order correction for residual interference from O<sub>2</sub> LIF has been performed by using spectrally resolved emission measurements of the flame. Further understanding of spectral features exhibited by CO<sub>2</sub> will be required to enable a more detailed and quantified isolation of the O<sub>2</sub> contribution.

The CO<sub>2</sub> excitation is strongly temperature-dependent, and this visualization strategy will isolate the high temperature regions of the combustion effluent, possibly proving a measurement strategy to directly infer temperature in flames with uniform CO<sub>2</sub> concentrations. The strategy reported here for UV visualization of high-temperature CO<sub>2</sub> in high-pressure combustion exhaust may also prove very useful to understand mixing phenomena in a variety of practical combustion devices.

Further work is underway to image CO<sub>2</sub> at higher pressures (~ 60 bar) and to quantify the temperature and wavelength-dependence of the CO<sub>2</sub> fluorescence quantum yield. In addition, fundamental spectroscopic study of hot CO<sub>2</sub> interaction with UV light is currently void and should be addressed. It should also be noted that correction methods utilized in the current study are limited to stable flames, and additional investigation into single shot measurement techniques are also being addressed.

**ACKNOWLEDGEMENTS** Work at Stanford was supported by the Air Force Office of Scientific Research (AFOSR), Aerospace and Materials Science Directorate, with Dr. Julian Tishkoff as technical monitor. The Division of In-

ternational Programs at the US National Science Foundation supports the Stanford collaboration via a cooperative research grant. The University of Heidelberg work and travel are sponsored by the Deutsche Forschungsgemeinschaft (DFG) and the Deutsche Akademische Auslandsdienst (DAAD).

#### REFERENCES

- 1 K. Kohse-Höinghaus, J.B. Jeffries (Eds.): *Applied Combustion Diagnostics* (Taylor, Francis, NY 2002)
- 2 A.C. Eckbreth: *Laser Diagnostics for Combustion, Temperature, and Species* (2nd edn., Gordon, Breach, Amsterdam, The Netherlands 1996)
- 3 J.C. Wolfrum: Proc. Combust. Inst. **27**, 1 (1998)
- 4 C.D. Carter, J.M. Donbar, G.S. Elliot: Proc. ASME Flu. Eng. Div. **258**, 3 (2002)
- 5 H. Werner: Proc. Comb. Inst. **28**, 1119 (2000)
- 6 F. Hildenbrand, C. Schulz, V. Sick, E. Wagner: Appl. Opt. **38**, 1452 (1999)
- 7 J.E. Dec, R.E. Canaan: SAE 980147 (Soc. Automotive Engineers, Warrendale, Pa. 1998)
- 8 B.J. Kirby, R.K. Hanson: Appl. Opt. **40**, 6136 (2002)
- 9 B.J. Kirby, R.K. Hanson: Appl. Opt. **41**, 1190 (2002)
- 10 C. Schulz, J.D. Koch, D.F. Davidson, J.B. Jeffries, R.K. Hanson: Chem. Phys. Lett. **355**, 82 (2002)
- 11 C. Schulz, J.B. Jeffries, D.F. Davidson, J.D. Koch, J. Wolfrum, R.K. Hanson: Proc. Combust. Inst. **29**, 2725 (2002)
- 12 W.G. Bessler, C. Schulz, T. Lee, J.B. Jeffries, R.K. Hanson: Chem. Phys. Lett. **375**, 344 (2003)
- 13 G. Herzberg: *Spectra of Diatomic Molecules*, Vol. 1 Molec. Spectra and Molec. Struc. (Krieger, Malabar, Fla. 1950)
- 14 W.G. Bessler, C. Schulz, T. Lee, J.B. Jeffries, R.K. Hanson: Appl. Opt. **42**, 24 (2003)
- 15 W.G. Bessler, C. Schulz, V. Sick, J.W. Daily: 3rd Joint Meeting US Sec. Combust. Inst., Chicago (2003) <http://www.lifsim.com>
- 16 W.G. Bessler, C. Schulz, T. Lee, D.-I. Shin, M. Hofmann, J.B. Jeffries, J. Wolfrum, R.K. Hanson: Appl. Phys. B **75**, 97 (2002)
- 17 W.G. Bessler, C. Schulz: Appl. Phys. B **78**, 519 (2004)